Application of Hamilton Principle in the control of Tethered Satellite System Pendular Motion

Paul TIROP*,[1], Zhang JINGRUI[1]

*Corresponding author
[1]Beijing Institute of Technology,
No. 5 Zhongguancun Street, Haidian District, Beijing, 100081, China,
paultirop@yahoo.com*, zhangjingrui@bit.edu.cn

DOI: 10.13111/2066-8201.2018.10.2.10

Received: 15 November 2017/ Accepted: 16 January 2018/ Published: June 2018

Aerospace Europe CEAS 2017 Conference,
16th-20th October 2017, Palace of the Parliament, Bucharest, Romania
Technical session Satellite Communications

Abstract: *The control of a tethered satellite system pendular motion is done by application of Hamiltonian equation of motion on a control design method known as planar H tracking. In this case, the reference motion is considered a natural planar motion. The control of the TSS is accomplished by using the inside plane control inputs as well as the outside plane control inputs. The designed control laws are able to drive the pendular motion to a natural planar trajectory with the required characteristics. The control inputs are analyzed using their magnitude ability. The numerical simulation results for each control inputs show that the inside of plane input not only has strong magnitude, but also effectively controls the pendular motion of the tethered satellite system.*

Key Words: *Tethered Satellite System, Hamiltonian equation, Control laws, Pendular motion*

1. INTRODUCTION

With a rise in modern technology, cheap, effective and reliable control designs are the main focus of research in Tethered Satellite Systems (TSS). Generally, the dynamics and control of tethered satellites are very complicated. The tethers are normally susceptible to undergo a complicated set of vibrations and librations during satellite operations in a space environment [1]. This problem becomes challenging during the deployment and retrieval of the TSS as a result of the presence of Coriolis accelerations [2]. Motions with large amplitudes may result in high tensional stress that is beyond the stress of the tether which may at the end result to the tether failure. From the point of view of tether control, the performance requirements in TSS are often quite demanding [3] and therefore the most important idea in TSS is how to apply the control action to the system [4, 5]. Any control system has to be designed according to the needs of a specified mission. A dump-bell system is the simplest model of the TSS.

It is composed of a group of massive bodies connected by massless tethers with the satellite attitude dynamics and the tether flexibility, both being ignored [6]. In a TSS two or more satellites are attached to each other to portray high dynamic potential in various applications [7]. This is seen from the work of Tsiolkovsky in 1895 [8]. There are other so many published literatures on the dynamic and control of TSS [9 - 15]. Belotsky and Levin did a

very impressive job [9]. Rupp also proposed a valuable tension control law which is used up to date [10]. New authors have come up with their ideas on control of TSS. Krupa *et al* [16] discussed on the dynamics and control of two bodies TSS based on the Finite Element Method. Takaechi et al [17] studied about the periodic solution of libration motions of the TSS in an elliptic orbit and ended up devising a controller known as "on – off" that could drive the system to periodic libration trajectories.

Another writer by the name of Barko et al [18] discussed on the control of deployed tether satellites through the comparison of six different strategies which include: (1) free deployment only due to the gravity gradient vector, (2) force braked deployment, (3) Kissel's law using a linear proportional derivative (PD) controller, (4) open-loop time-optimal control, (5) pendulum control, and (6) targeting and stabilization following the controlling chaos strategy. Steindl *et al.* [19, 20] come up with the optimal controllers to achieve effective controlled deployment and retrieval of a TSS based on the multiple shooting method.

Williams and Trivailo [21] extended their investigations on optimal control to the controlling of the librations of a TSS in elliptic orbits by tracking periodic libration trajectories [22]. Linear Quadratic (LQ) and proportional integral derivative (PID) control methods were first used in flying system formation [23 - 25].

In this paper, the description of the system is first made. Then the equations of motion for the end body, the tether and the sub-body are derived. The equations that will control the pendular motion of the TSS are further achieved. Finally, Hamiltonian equation of the pendular motion is used together with a design method referred to as planar H tracking. The control laws are first made so that they are used to drive the TSS pendular motion to track a natural planar reference trajectory. The control is accomplished using the in-plane control inputs and out-plane control inputs. The simulation results for each control inputs are obtained in response to the system response for H planar control design and the control inputs. The efficiency of control in the two planes is determined by the level of their magnitude.

2. SYSTEM DESCRIPTION

The system is composed of a centered body (earth), end body (deploy / base satellite), sub – body (sub satellite) and a cable (tether) as presented in Fig. 1.

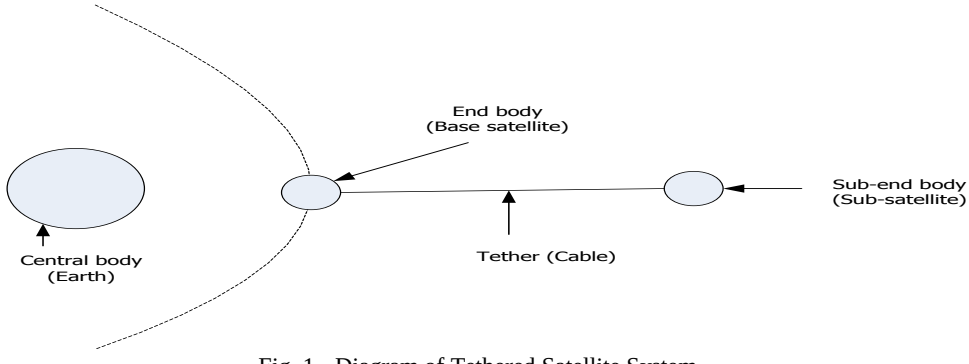

Fig. 1 - Diagram of Tethered Satellite System

From the description of the system, modelling assumptions are made in relation to the physical environment of the system. The first assumption made is that the central body (earth) is sphered shaped and it represents itself as a point mass. The second assumption

states that the magnetic field is a tilted di-pole fixed at the center of the central body as it keeps on rotating. The final assumption is that the gravitational force of the central body and electrodynamic forces are external forces that act on the system. This implies that the gravity of the central body and other components such as drag and solar radiations are negligible in the system. In TSS, modeling assumptions can be outlined as follows:
a) The end body and the sub-body are finite rigid bodies.
b) The tether is an elastic string that can resist axial stretching (it can't support compression and has negligible torsion and bending characteristics).

3. EQUATION OF MOTION

A mathematical model of the system is created by using the modelling assumptions that were outlined in Section 2. Figures of the central body (CB), end body (E) and the sub-body (S) are illustrated together with their frame coordinates in Fig. 2.
The state of the end body E is used as the orbital motion of the system. It is parameterized by osculating classical elements of the orbit [26] as shown below.

$$e = (a\ell\Omega \mathrm{I}\omega\nu)^T \tag{1}$$

The distance from the center O of the central body C to the mass center G_E of the end body E is $\vec{r}_E$ The distance from the mass center of the end body E to the point of tether N_E attachment is $\vec{N}_E$ whereas dl, is the differential tether length with arc length l from point N_E in the end body E to point N_S in the sub–end body S. The point N_S relative to mass center of the sub-end body S is given as $\vec{N}_S$. The coordinate frames of each body are shown in Fig. 2, and Fig. 3.

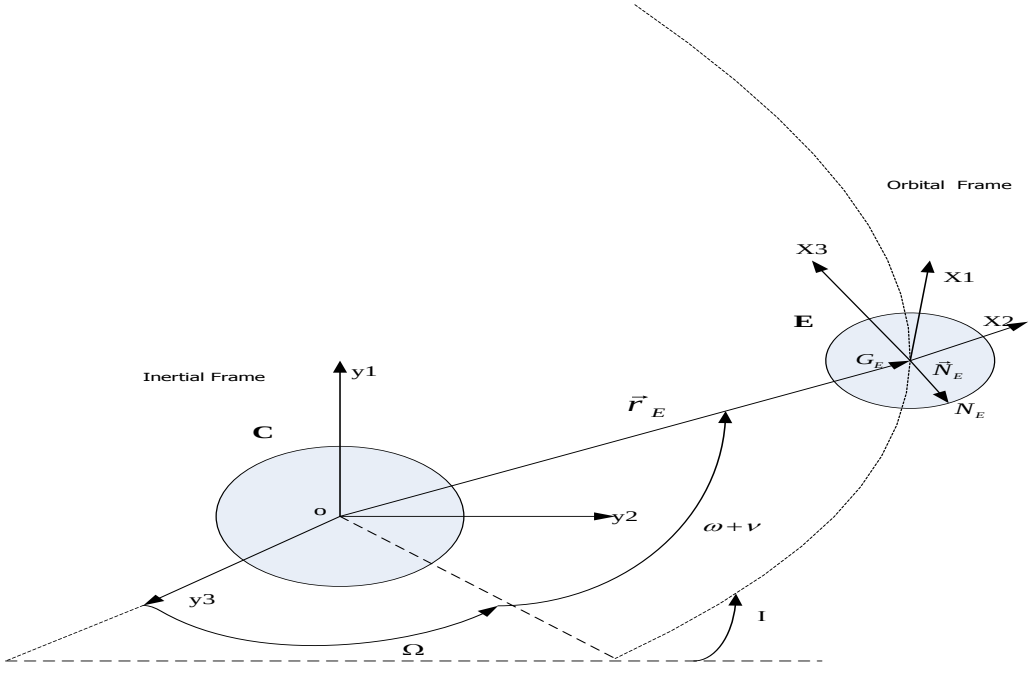

Fig. 2 - Coordinate diagram of the central body C and the end body E

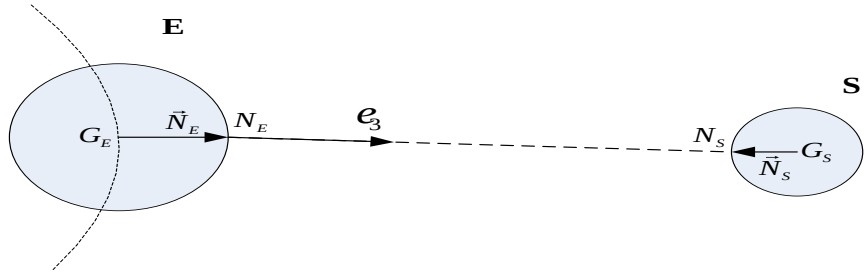

Fig. 3 - Diagram of the end body E and Sub-end body S

Inertial frame on the central body C with the denotation F_I has coordinates yi and a central position O, $y3$ axes on the inertial frame lies on the spin axis of the central body C. The $y1-y2$ axis creates a plane that corresponds to the Equatorial plane of C.

Orbital frame F_O of instanteneous Keplerian orbit of G_E (end body E) has coordinate axes xi. The $x3$ axis is derived from the center O of the central body C to G_E, whereas $x2$ is pointing to the direction of the instantaneous angular momentum of the Keplerian orbit. The final axis $x1$ completes the right-hand triad. On performing 3-1-3 Euler rotation [27] through the angles Ω, I and $\lambda = \omega + \nu$, the inertial frame is changed to orbital frame. The directional cosine matrix (DCM) that connects the inertial frame with the orbital frame is represented as:

$$R^{EO} = \begin{pmatrix} \cos\alpha & 0 & -\sin\alpha \\ -\sin\alpha\sin\beta & \cos\beta & -\cos\alpha\sin\beta \\ \sin\alpha\cos\beta & \sin\beta & \cos\alpha\cos\beta \end{pmatrix} \tag{2}$$

The acceleration and angular velocities of orbital frame F_0 in relation to the inertial frame F_I are presented as:

$$\vec{\omega}_{O/I} = \frac{\sqrt{\mu P}}{r_E^3} y2 \tag{3}$$

$$\dot{\vec{\omega}}_{O/I} = \frac{2\mu\sin\nu}{r_A^3} x2 \tag{4}$$

μ - Gravitational parameter of the central body C

$$P = a(1-e^2) \tag{5}$$

$$r_A = \frac{P}{1+e\cos\nu} \tag{6}$$

P is the orbital parameter whereas r_A is the instantaneous orbit radius of the mass centre end body S.

3.1 Equations of motion of the end body E

It consists of the following equations:

a) Equation governing the evolution of the instantaneous keplerian orbit of mass center G_E of the end body E
b) Equations governing the rotation of the fixed body coordinate frame F_E in relation to F_O
Orbital equations for G_E are done by application of Newton's second law [28] to the end body E thus:

$$m_E \ddot{\vec{r}}_E = \vec{F}_{GE} + \vec{T}(0,t) \tag{7}$$

m_E is Mass of the end body E; $\vec{F}_{GE}$ is the Gravitational force of the central body acting on the end body E whereas $\vec{T}(0,t)$ is the Tether tension on the end body E at the point N_E.
From the physical assumptions made in Section 1, the central body is treated as appoint mass. This implies that:

$$\vec{F}_{GE} = -\frac{m_E \mu}{r_E^3} \vec{r}_E \tag{8}$$

The Eq. (8) above is known as the Newton's law of universal gravitation. Applying Eq. (8) to Eq. (7), Orbital equation of motion for G_E is achieved and presented as:

$$\ddot{\vec{r}}_E = -\frac{\mu}{r_E^3} \vec{r}_E + \frac{\vec{T}(0,\mathrm{t})}{m_E} \tag{9}$$

For the rotational equation of the end body E, Euler rotational equation is applied.

$$\vec{\mathrm{I}}_E \cdot \dot{\vec{\omega}}_{E/I} + \vec{\omega}_{E/I} \times \vec{\mathrm{I}}_E \cdot \vec{\omega}_{E/I} = \vec{M}_{GE} + \vec{P}_E \times \vec{T}(0,t) \tag{10}$$

$\vec{\mathrm{I}}_E$ is the Centroid moment of inertia tensor of the end body E
$\vec{\omega}_{E/I}$ is the Angular velocity of a fixed body principal coordinates F_E of the end body E in relation to the F_I

$$\vec{\omega}_{E/I} = \vec{\omega}_{E/O} + \vec{\omega}_{O/I} \tag{11}$$

$\vec{M}_{GE}$ is the Gravity gradient torque acting on the end body E at its mass center.
By using linear approximation of gradient torque [29, 30]:

$$\vec{M}_{GE} = \frac{3\mu}{r_E^5} \vec{r}_E \times \vec{\mathrm{I}}_E \cdot \vec{r}_E \tag{12}$$

Substituting $\vec{M}_{GE}$ in Eq. (10) with the results from Eq. (12):

$$\vec{\mathrm{I}}_E \cdot \dot{\vec{\omega}}_{E/I} + \vec{\omega}_{E/I} \times \vec{\mathrm{I}}_E \cdot \vec{\omega}_{E/I} = \frac{3\mu}{r_E^5} \vec{r}_E \times \vec{\mathrm{I}}_E \cdot \vec{r} + \vec{P}_E \times \vec{T}(0,t) \tag{13}$$

The above Eq. (13) represents the rotational equation of motion of the end body E.

3.2 Equations of motion of the end body S

Using Euler's rotational equation, the attitude equation of the sub-end body S is presented as:

$$\vec{\mathrm{I}}_S \cdot \dot{\vec{\omega}}_{S/I} + \vec{\omega}_{S/I} \times \vec{\mathrm{I}}_S \cdot \vec{\omega}_{S/I} = \vec{M}_{GS} - \vec{P}_S \times \vec{T}(L,t) \tag{14}$$

$\vec{\mathrm{I}}_S$ is the Centroid moment of inertia tensor for the sub-body S; $\vec{\omega}_{S/I}$ - Angular velocity of sub-end body coordinate frame F_S in relation to F_I and $\vec{M}_{GS}$ - Gravity gradient torque

$$\vec{\omega}_{S/I} = \vec{\omega}_{S/O} + \vec{\omega}_{O/I} \tag{15}$$

$$\vec{M}_{GS} = \frac{3\mu}{r_S^5} \vec{r}_S \times \vec{\mathrm{I}}_S \cdot \vec{r}_S \tag{16}$$

Substituting gravity gradient torque $\vec{M}_{GS}$ in Eq. (16) to Eq. (14):

$$\vec{\mathrm{I}}_S \cdot \dot{\vec{\omega}}_{S/I} + \vec{\omega}_{S/I} \times \vec{\mathrm{I}}_S \cdot \vec{\omega}_{S/I} = \frac{3\mu}{r_S^5} \vec{r}_S \times \vec{\mathrm{I}}_S \cdot \vec{r}_S - \vec{P}_S \times \vec{T}(L,t) \tag{17}$$

The above Eq. (17) represents the rotational equation of motion of the sub-end body S

3.3 Pendular equations of motion

Using the assumptions from the physical model, it is assumed that in the pendular equation of motion the elastic vibration of the tether does not affect the pendular motion of the TSS and the tether is a rigid body. The equations that are to control the pendular motion of the TSS are achieved by the application of Euler equation of rigid body dynamics. It is a first order ordinary differential equation describing the rigid body.

$$\mathrm{I} \cdot \dot{\omega} + \omega_x (\mathrm{I} \cdot \omega) = M \tag{18}$$

M - Applied rotation; I - Inertia rotation; ω - Angular velocity on the principle axis
For an end body E the Euler's rotational equitation will be as follows:

$$\vec{\mathrm{I}}_E \cdot \dot{\vec{\omega}}_{E/I} + \vec{\omega}_{E/I} \times \mathrm{I}_E \cdot \vec{\omega}_{E/I} = \vec{M}_E \tag{19}$$

$\vec{\mathrm{I}}_E$ - Moment of inertia tensor; $\vec{M}_E$ - Total external moment
The moment of inertia tensor is expressed as follows:

$$\vec{\mathrm{I}}_E = \mathrm{I}_E (1 - e_3 e_3) \tag{20}$$

This is because the mass of the system lies on the axis.
I_E - Scalar moment of inertia; 1- Identity tensor
By combining the equation of the angular velocity of a tethered fixed coordinate frame (F_E) to the orbital frame (F_O) coordinate the following equation is achieved.

$$\vec{\omega}_{E/O} = \dot{\beta}_{e_1} + \dot{\alpha} \cos \beta_{e_2} + \dot{\alpha} \sin \beta_{e_3} \tag{21}$$

With angular velocity of the orbital coordinate in place, then it relates to the inertial coordinate frame (F_I) as:

$$\vec{\omega}_{O/I} = \Omega_A O_2 \tag{22}$$

Ω_A - Constant angular rate

The equations of the angular velocity and acceleration of tether fixed coordinate frame in relation to inertial frame will be presented as shown below:

$$\begin{aligned}\vec{\omega}_{E/I} &= -\dot{\beta}_{e_1} + (\dot{\alpha}+\Omega_A)\cos\beta_{e_2} + (\dot{\alpha}+\Omega_A)\sin\beta_{e_3} \\ \dot{\vec{\omega}}_{E/I} &= -\ddot{\beta}_{e_1} + [\ddot{\alpha}\cos\beta - (\dot{\alpha}+\Omega_A)\dot{\beta}\sin\beta]e_2 + [\ddot{\alpha}\sin\beta + (\dot{\alpha}+\Omega_A)\dot{\beta}\cos\beta]_{e_3}\end{aligned} \tag{23}$$

In this situation $\vec{M}_A$ is as a result of gravity-gradient acting on the system. The length of the system appears to be smaller than the orbital radius. Due to this aspect, linear approximation for gravity gradient torque method is used [29]. This method is represented as:

$$\vec{M}_A = 3\Omega_A^2 O_3 \times I_A \cdot O_3 \tag{24}$$

By combining all these formulas together, the equation of pendular motion is achieved, such that the equation will appear as represented bellow:

$$\begin{aligned}&\ddot{\alpha}\cos\beta - 2(\dot{\alpha}+\Omega_A)\dot{\beta}\sin\beta + 3\Omega_A^2\sin\alpha\cos\alpha\cos\beta = 0 \\ &\ddot{\beta} + [(\dot{\alpha}+\Omega_A)^2 + 3\Omega_A^2\cos^2\alpha]\sin\beta\cos\beta = 0\end{aligned} \tag{25}$$

This equation is the same as of the dumb-bell satellite, which can also provide a simplified solution to the existing problem.

3.4 Application of Hamiltonian principle

The equation (25) above, describing the inside plane pendular motion is confined to a non-dimensional form by defining the non-dimensional time with the boundary conditions as represented in the following equations.

$$\begin{aligned}&u(0,t) = u(L,\mathrm{t}) \\ &\mathrm{v}(0,\mathrm{t}) = \mathrm{v}(\mathrm{L},\mathrm{t}) = 0 \\ &t = \frac{\tau}{\Omega_A}\end{aligned} \tag{26}$$

τ - The angle in which the end body moves in the circular orbit; t - Time; Ω_A - Constant angular rate

The pendular equation of motion will be in a non-dimensional form which will appear as:

$$\begin{aligned}&\ddot{\alpha}\cos\beta - 2(\dot{\alpha}+1)\dot{\beta}\sin\beta + 3\sin\alpha\cos\alpha\cos\beta = 0 \\ &\ddot{\beta} + \left[(\dot{\alpha}+1)^2 + 3\cos^2\alpha\right]\sin\beta\cos\beta = 0\end{aligned} \tag{27}$$

The above equations of the pendular motion are linearized such that the nominal pendular motion of the tether will appear as a planar spinning on the angles $\beta = \dot{\beta} = 0$ which is represented in the form of the equation below.

$$\begin{aligned}&\ddot{\alpha}\cos\beta - 2(\dot{\alpha}+1)\dot{\beta}\sin\beta + 3\sin\alpha\cos\alpha\cos\beta = 0 \\ &\ddot{\beta} + \left[(\dot{\alpha}+1)^2 + 3\cos^2\alpha\right]\sin\beta\cos\beta = 0\end{aligned} \tag{28}$$

The solution for an inside plane motion is obtained by integrating the equation (28), such that it will appear as represented bellow:

$$\dot{\alpha} = \pm\sqrt{h - 3\sin^2}\alpha \tag{29}$$

$(+)$ Systems with positive angular rate; $(-)$ Systems with negative angular rate; $h-$

Constant simplified version of the Hamiltonian of the pendular motion [29]. The Hamiltonian equation is represented as shown below.

$$H = (\dot{\alpha}^2 + 3\sin^2\alpha)\cos^2\beta + \dot{\beta}^2 + 4\sin^2\beta \tag{30}$$

Linearizing the above Hamiltonian equation (30) for small out-of- plane angle β, the equation of the pendular motion is achieved and presented as follows:

$$\ddot{\alpha}\cos\beta - 2(\dot{\alpha} + \Omega_A)\dot{\beta}\sin\beta + 3\Omega_A^3\sin\alpha\cos\alpha\cos\beta = 0 \tag{31}$$

The pendular motion in this case is a planar. These mean that $H = h$.

The objective of Hamiltonian planar tracking control design [31 - 34] is to drive β and $\dot{\beta}$ to Zero value, while at the same time driving H to a certain desired value h^*. The final result is a natural planar motion in the form of $h = h^*$ As it appears that the out-of-plane motion is driven to zero, then the control law for u_β is given as:

$$u_\beta = -k_{\beta 1}\beta - k_{\beta 2}\dot{\beta} + \left[(\dot{\alpha}+1)^2 + 3\cos^2\alpha\right]\sin\beta\cos\beta \tag{32}$$

$k_{\beta 2} > 0$; Therefore the closed loop equation will be:

$$\ddot{\beta} + k_{\beta 2}\dot{\beta} + k_{\beta 1}\beta = 0 \tag{33}$$

Given an assumption that the arbitrary control inputs corresponding to u_α and u_β are provided by small thrusters at the sub-body B, then the equation governing the pendular motion of the tether will be presented as:

$$\begin{aligned} u_\alpha &= \ddot{\alpha}\cos\beta - 2(\dot{\alpha}+1)\dot{\beta}\sin\beta + 3\sin\alpha\cos\alpha\cos\beta \\ u_\beta &= \ddot{\beta} + \left[(\dot{\alpha}+1)^2 + 3\cos^2\alpha\right]\sin\beta\cos\beta \end{aligned} \tag{34}$$

By differentiating equation (30) using equation (34), it is observed that the time rate of change of H will be as follows:

$$\dot{H} = 2\left(\dot{\alpha}u_\alpha\cos\beta + \dot{\beta}u_\beta\right) \tag{35}$$

$$u_\alpha = -\frac{1}{\dot{\alpha}\cos\beta}\left[\frac{k_H\left(H - h^*\right)}{2} + \dot{\beta}u_\beta\right] \tag{36}$$

Eq. (36) shows the control law of u_α, where: $k_H > 0$ - is the constant control gain. Substituting the Eq. (36) into Eq. (35), the closed loop dynamics of H will be:

$$k_H h^* = \dot{H} + k_H H \tag{37}$$

From equation (36), k_H appears to be positive. The control law in equation (36) drives H to h^* exponentially as the angle in which the body moves (τ) approaches infinity.

4. NUMERICAL SIMULATION

The initial conditions used to generate the graphical presentations are;
$\alpha = 0; \dot{\alpha} = 2.375; \beta = 0.3; \dot{\beta} = 0$

The parameters used are: $h^* = 20; k_{\beta 2} = \frac{\ln(100)}{2\pi}; k_{\beta 1} = \frac{k_{\beta 1}^2}{4}; k_H = -\frac{\ln(100)}{2\pi}$

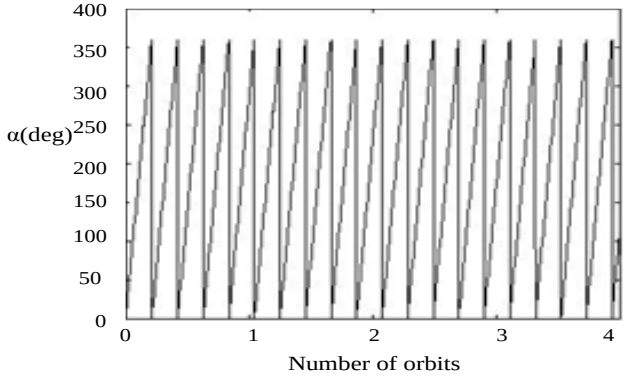

(a) Inside of plane angle

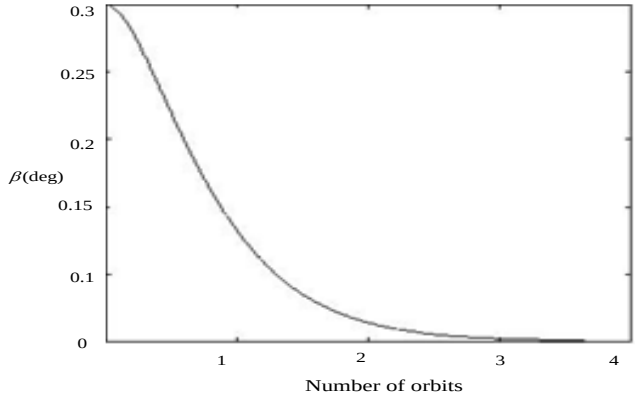

(b) Outside of plane angle

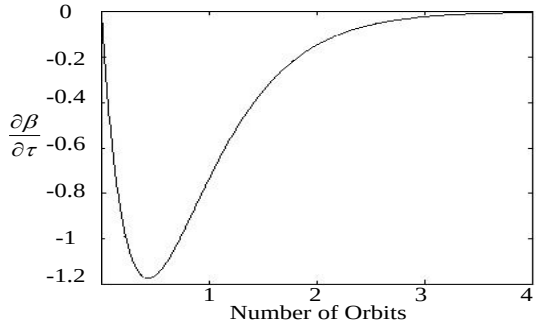

(c) Outside of plane angular rate

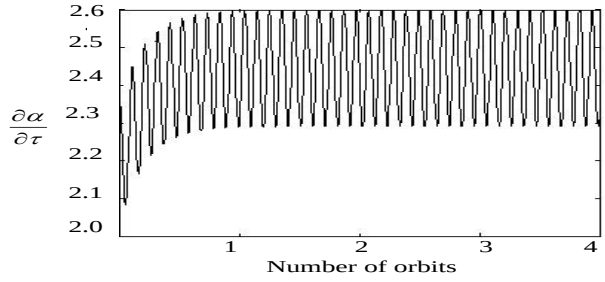

(d) Inside of plane angular rate

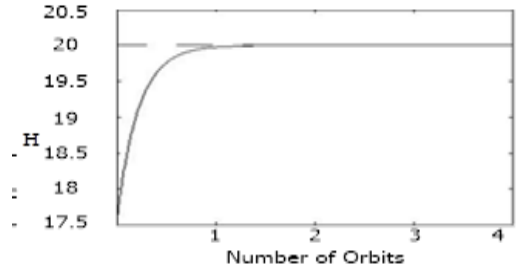

(e) Planar H

Fig. 4 - The above graphs are for the system response for planar H tracking.

Fig. 4 shows that the control laws applied are successful in driving the pendular motion to a desired natural planar trajectory with $h = h^*$ .This fact is shown in Fig. 4 (b), 4 (c) and 4(e) in which the out- of –plane motion and the quantity H do not undergo any amplitude oscillations about the desired reference motion.

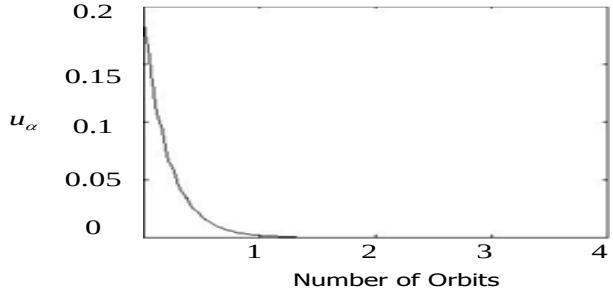

(a) inside of plane control inputs

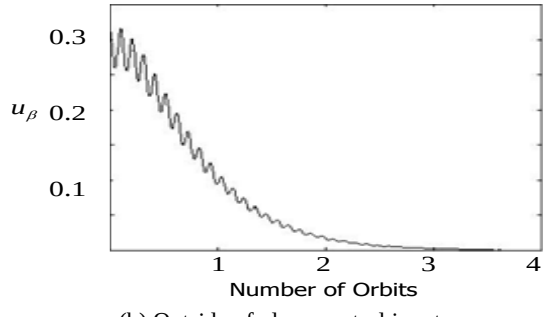

(b) Outside of plane control input

Fig. 5 - The above graphs (a) and (b) represent the Control inputs for planar H control tracking

In Fig. 5, u_α and u_β both do approach zero as the maneuvers are completed. This implies that the propellant required in performing the maneuvers decreased significantly as the maneuvers approached completion. The magnitude of u_α is seen to be significantly smaller which is the primary advantage of the H tracking control law. The in plane control input is also lower because of the qualitative characteristics of the reference motions.

5. CONCLUSIONS

In this work, the application of Hamiltonian principle has been studied to enable the control of pendular motion of the TSS in an elliptic orbit. The tether system considered in the study is based on the classical dumbbell model. It is assumed that the end-body and the sub- end body are finite rigid bodies and that also the tether is an elastic string that could resist axial stretching. The mathematical model developed in the paper, assists in the formation of the equations of motions for both the end and sub-end bodies. The pendular equations of motions are achieved by the application of Euler equation of the rigid bodies using the assumptions previously highlighted. The control laws are developed to drive the pendular motion to a preferred natural trajectory. Numerical simulations of the controlled pendular motion of the tether showed that the control laws used were successful in driving the pendular motion of the tether to a natural planar trajectory. It was seen that the magnitude of u_α in the inside plane was significantly smaller than that of u_β in the outside plane. The in-plane control input was also lower because of the qualitative characteristics of the reference motion. This became the primary advantage of Hamiltonian Principle in the control of the Pendular motion in a TSS. However, the major disadvantage was in tracking a specific time history for α, that could be needed somewhere else because this method requires a less precise control. In that case, some other methods of control must be employed that will require more precise control. This idea leads in the development of more precise control methods in future that could efficiently control the TSS.

REFERENCES

[1] J. Peláez, E. C. Lorenzini, O. Lopez-Rebollal, et al., A new kind of dynamic instability in electrodynamic tethers, *Journal of Astronautical Science*, vol. **48**, no.4, pp. 449–476, 2000.

[2] J. A. Carroll, *Guidebook for Analysis of Tether Applications*, National Aeronautics and Space Administration, Springfield, VA, 1985.

[3] C. Menon, C. Bombardelli, Self-stabilising attitude control for spinning tethered formations, *Acta Astronautica*, vol. **60**, no.10–11, pp. 828–833, 2007.

[4] K. D. Kumar, Review of dynamics and control of non-electrodynamic tethered satellite Systems, *Journal of Spacecraft and Rockets*, vol. **43**, no.4, pp. 705–720, 2006.

[5] M. P. Cartmell, D. J. Mckenzie, A review of space tether research, *Progress in Aerospace Sciences*, vol. **44**, no.1, pp. 1– 21, 2008.

[6] H. Wen, D. P. Jin, H. Y. Hu, Optimal feedback control of the deployment of a tethered Sub-satellite subject to perturbations, *Nonlinear Dynamics*, vol. **51**, no.4, pp. 501–514, 2008.

[7] P. M. Bainum, K. S. Evans, Three- dimensional motion and stability of two rotating Cable-connected bodies, *Journal of Spacecraft and Rockets*, vol. **12**, no.4, pp. 242- 250, 1975.

[8] V. V. Beletsky and E. M. Levin, Dynamics of Space Tether Systems, *Advances of Astronautical Sciences*, vol.**83**, pp. 267 – 322, 1993.

[9] Y. Chen, R. Huang, L. He, X. Ren, B. Zheng, Dynamical modelling and control of space Tethers, a review of space tether research, *Nonlinear Dynamics*, vol. **77,** no.4, PP. 1077 – 1099, 2014.

[10] A. K. Misra, V. J. Modi, Dynamics and Control of Tethered connected two- body systems, brief review, *proceedings of Paris International Astronautics Federation Congress*, **1**, France, 1982.

[11] P. Williams, A review of space tether technology, *Recent Patent on Space Technology*, vol. **2**, no.1, pp. 22 – 36, 2012.
[12] A. A. T. Hong, R. Varathatajoo, F. Romli, Analytic solutions for Tethered Satellite Systems (TSS) subject to internal and external torques undergoing a spin – up and spin – down Maneuvers, *Aircraft Engineering and Aerospace Technology*, vol. **87**, no.6, pp. 514 – 520, 2015.
[13] M. P. Cartmoll and D. J. Mckenzie, A review of space tether research, *Progress in Aerospace Sciences*, vol. **44**, no.1, pp. 1 – 21, 2008.
[14] M. L. Cosmo, E. C. Lorenzini, *Tethers in Space Handbook*, NASA, Washington D.C.
[15] J. R. Ellis, C. D. Hall, Out-of-plane librations of spinning tethered satellite systems, *Celestial Mechanics and Dynamical Astronomy*, vol. **106**, no.1, pp. 39 – 67, 2010.
[16] M. Krupa, W. Poth, M. Schagerl, et al., Modelling, dynamics and control of tethered satellite systems, *Nonlinear Dynamics*, vol. **43**, no. 1–2, pp. 73–96, 2006.
[17] N. Takeichi, M. C. Natori, N. Okuizumi, et al., Periodic solutions and controls of tethered systems in elliptic orbits, *Journal of Vibrations, Control and Dynamics*, vol. **10**, no. 10, pp. 1393–1413, 2004.
[18] B. Barkow, A. Steindl, H. Troger, A targeting strategy for the deployment of a tethered satellite system, *IMA Journal of Applied Mathematics*, vol. **70**, no.5, pp. 626–644, 2005.
[19] A. Steindler, H. Troger,Optimal control of deployment of a tethered sub-satellite, *Nonlinear Dynamic*, vol. **31**, no.3, pp. 257–274, 2003.
[20] A. Steindler, W. Steiner, H. Troger, Optimal control of retrieval of a tethered Sub-satellite, *Applied Solid Mechanics*, vol. **122**, pp. 441–450, 2005.
[21] P. Williams, P. Trivailo, On the optimal deployment and retrieval of tethered satellites, In: *The 41st AIAA/ASME/SAE/ASEE Joint Propulsion Conference and Exhibit*, Tucson, July 10–13, 2005.
[22] P. Williams, Libration control of tethered satellites in elliptical orbits, *Journal of Spacecraft and Rockets*, vol. **43**, no. 2, pp.476–479, 2006.
[23] B. Barkow, A. Steindl, H. Troger, G. Wildermann, Various methods of controlling the deployment of a Tethered Satellite, *Journal of Vibration and Control*, vol. **9**, no.23, pp. 187 – 208, 2003.
[24] J. D. Pearson, Approximation methods in optimal control and sub – optimal control, *Journal of Electronics and Control*, vol. **13**, no.5, pp. 453 – 469, Received 30 May 1962, Published online: 27 Apr 2007.
[25] G. Andrikopoulos, G. Nnikolakopoulos, S. Manesis, Experimental constrained optimal Attitude Control of a Quadrator subject to wind disturbances, *IEEE, Transactions of Industrial Electronics*, 2014.
[26] F. R. Moulton, *Introduction to Celestial Mechanics*, *Mineola*, New York, 1970.
[27] R. H. Battin, *An introduction to the mathematics and methods of Astrodynamics*, AIAA, Reston, VA, 1999.
[28] V. I. Arnold, *Mathematical Methods of Classical Mechanics*, Springer – Verlag, New York, 1978.
[29] H. Schaub, J. L. Jenkins, Analytic Mechanics of Space Systems; Second Edition, AIAA, Reston, VA, 2009.
[30] P. C. Hughes, *Spacecraft Attitude Dynamics*, Dover, Mineola, New York, 1986.
[31] V. I. Arnold, Hamiltonian nature of Euler equations in the dynamics of rigid body and of a perfect fluid, *Usp. Mat Nauk*; vol. **24**, pp. 225 – 260, 1965.
[32] A. H. Boozer, *Magnetic field line Hamiltonian*, Princeton Plasma Phys. Lab, PPPL-2094R, 1985.
[33] M. G. Calkin, *Langrangian and Hamiltonian Mechanics*, World Scientific, New Jersey, 1996.
[34] W. R. Hamilton, *Hamilton Principle and Physical Systems*, Academic Press, New York, 1967.